J. Fluid Mech. (2023), *vol*. 956, A7, doi:10.1017/jfm.2023.6

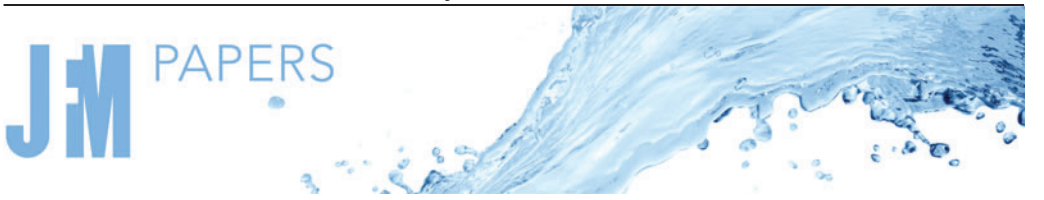

Critical balance and scaling of strongly stratified turbulence at low Prandtl number

Valentin A. Skoutnev†

Department of Astrophysical Sciences, Princeton University, Princeton, NJ 08544, USA

(Received 8 May 2022; revised 10 November 2022; accepted 21 December 2022)

We extend the scaling relations of strongly (stably) stratified turbulence from the geophysical regime of unity Prandtl number to the astrophysical regime of extremely small Prandtl number applicable to stably stratified regions of stars and gas giants. A transition to a new turbulent regime is found to occur when the Prandtl number drops below the inverse of the buoyancy Reynolds number, i.e. $Pr\,Rb < 1$, which signals a shift of the dominant balance in the buoyancy equation. Application of critical balance arguments then derives new predictions for the anisotropic energy spectrum and dominant balance of the Boussinesq equations in the $Pr\,Rb \ll 1$ regime. We find that all the standard scaling relations from the unity Pr limit of strongly stratified turbulence simply carry over if the Froude number, Fr, is replaced by a modified Froude number, $Fr_M \equiv Fr/(Pr\,Rb)^{1/4}$. The geophysical and astrophysical regimes are thus smoothly connected across the $Pr\,Rb = 1$ transition. Applications to vertical transport in stellar radiative zones and modification to the instability criterion for the small-scale dynamo are discussed.

Key words: stratified turbulence

1. Introduction

Turbulence in the strongly stratified regions of planetary oceans, atmospheres and the interiors of stars and gas giants provides an important source of vertical transport of chemicals and momentum, thereby playing a critical role in their long-term evolution (Zahn 1974, 1992; Fernando 1991; Pinsonneault 1997; Maeder & Meynet 2000; Ivey, Winters & Koseff 2008; Ferrari & Wunsch 2009; Aerts, Mathis & Rogers 2019; Garaud 2021). However, current understanding of the extremely low thermal-Prandtl-number regime of astrophysical turbulence remains disjoint from the order-unity Prandtl-number regime of geophysical turbulence. This is despite identical asymptotic limits for the Reynolds number ($Re \gg 1$), Froude number ($Fr \ll 1$) and buoyancy Reynolds number ($Rb = Re\,Fr^2 \gg 1$). The Prandtl number $Pr = \nu/\kappa$ measures the ratio of the microscopic

† Email address for correspondence: valentinskoutnev@gmail.com

© The Author(s), 2023. Published by Cambridge University Press

https://doi.org/10.1017/jfm.2023.6 Published online by Cambridge University Press

viscosity ν to the thermal diffusivity κ, and is extremely small in stellar plasma, in particular. Photons rapidly diffuse heat compared to the much slower momentum diffusion by ion–ion collisions, leading to $\kappa \gg \nu$. For reference, stellar radiative zones have Prandtl numbers that can range from $Pr = O(10^{-9})$ to at most $Pr = O(10^{-5})$, in contrast to Earth's fluids, which range from $Pr \simeq 0.7$ in the atmosphere to $Pr \simeq 10$ in the ocean (Garaud 2021). A Prandtl number as high as $Pr \simeq 700$ can be reached in parts of the ocean dominated by salt stratification (Thorpe 2005; Gregg *et al.* 2018; Gregg 2021) – where the salt diffusivity replaces thermal diffusivity. Compared to the $Pr = 1$ case, a small Pr can have significant effects on large-scale hydrodynamic instabilities and the resulting turbulence (Garaud 2021), while a large Pr influences scales comparable to and smaller than the viscous scale and can have significant effects on the buoyancy flux, mixing efficiency and properties of shear-induced turbulence (Salehipour, Peltier & Mashayek 2015; Legaspi & Waite 2020; Okino & Hanazaki 2020).

Many important features of the unity Prandtl-number regime are becoming better understood from a combination of numerical experiments (Waite & Bartello 2004; Brethouwer *et al.* 2007; Riley & Lindborg 2010; Maffioli & Davidson 2016; Lucas, Caulfield & Kerswell 2017; de Bruyn Kops & Riley 2019), observational data (Lindborg & Brethouwer 2007; Riley & Lindborg 2008; Falder, White & Caulfield 2016; Lefauve & Linden 2022) and theoretical developments (Billant & Chomaz 2001; Lindborg 2006; Chini *et al.* 2022). Strongly stratified turbulence with $Pr = O(1)$ forced at some horizontal length scale leads to emergent vertical scales set by the stratification and exhibits two distinct inertial ranges that transfer energy from the large forcing scales to the small viscous and thermal scales where it is dissipated. The transition length scale between the two ranges is known as the Ozmidov scale (Ozmidov 1992). The turbulence is highly anisotropic from the outer forcing scale down to the Ozmidov scale, with the down-scale energy transfer likely containing contributions from both a local energy cascade and non-local energy transfer mechanisms, e.g. shear instabilities, wave–wave interactions (Waite 2011; Augier, Billant & Chomaz 2015; Maffioli & Davidson 2016; Khani 2018). Below the Ozmidov scale, the turbulence is isotropic down to the diffusive scales. The properties of the energy cascade, relevant dimensionless parameters and scaling relations for the emergent vertical scales are now fairly well understood, although many further questions remain, such as on the efficiency of mixing (Gregg *et al.* 2018; Monismith, Koseff & White 2018; Legg 2021) and the origin of self-organized criticality (Smyth & Moum 2013; Salehipour, Peltier & Caulfield 2018; Smyth, Nash & Moum 2019; Chini *et al.* 2022; Lefauve & Linden 2022).

The main aim of this study is to extend the theoretical arguments used in the $Pr = O(1)$ regime to make analogous predictions for the emergent vertical scales and energy cascades in the asymptotically low Pr regime. If only the thermal diffusivity is increased while keeping all other parameters constant (thereby decreasing Pr), one should expect a smooth transition to occur between two asymptotic regimes when thermal diffusion shifts from being important only on the smallest viscous scales to playing an important role on the mesoscales, i.e. on scales comparable to or larger than the Ozmidov scale.

To understand this transition, we use the critical balance framework proposed by Nazarenko & Schekochihin (2011) for anisotropic wave systems. Critical balance argues that linear wave ω^{-1} and nonlinear interaction τ_{NL} time scales are comparable, $\omega^{-1} \sim \tau_{NL}$, on a scale-by-scale basis throughout a local energy cascade, giving a prediction for the anisotropy of the turbulence as a function of scale. Originally applied in mean-field magnetohydrodynamic (MHD) turbulence (Goldreich & Sridhar 1995) (see also Schekochihin (2022) and references therein), critical balance successfully

https://doi.org/10.1017/jfm.2023.6 Published online by Cambridge University Press

predicts power laws of the anisotropic energy spectra and associated transition scales in rotating turbulence and unity Prandtl-number strongly stratified turbulence (Nazarenko & Schekochihin 2011).

We propose that critical balance should naturally extend to low thermal-Prandtl-number strongly stratified turbulence with a modification in its physical interpretation. As Pr is decreased (by increasing κ while keeping ν small and fixed), the full internal gravity wave (IGW) dispersion ω smoothly transitions from the asymptotic dispersion for adiabatic, inviscid, propagating IGWs when $Pr = O(1)$ (i.e. $\omega \sim \omega_N$) to an asymptotic dispersion for overdamped, inviscid, IGWs modified by the interaction of buoyancy and fast thermal diffusion when $Pr \ll 1$ (i.e. $\omega \sim \omega_{lPe}$, where 'lPe' refers to the 'low turbulent Péclet-number' limit, as discussed in more detail in §§ 2 and 4). As a result, scaling laws for the emergent vertical scales and two cascades predicted by critical balance will likewise smoothly change as Pr is decreased. We note that, because critical balance assumes a local energy cascade, the relative role of non-local energy transfer mechanisms in the low Pr limit remains to be understood.

The paper layout is as follows. The Boussinesq equations used to model stably stratified turbulence are defined in § 2, followed by an argument for when a transition of turbulence regimes should occur. Critical balance arguments in the unity Pr regime are reviewed in § 3, which can then be compared with the new critical balance arguments in the low Pr regime given in § 4. Astrophysical applications of the new scaling laws are discussed in § 5.

2. The Boussinesq approximation and the $PrRb = 1$ transition

2.1. *The Boussinesq approximation*

Stably stratified regions of stars and gas giants below their surfaces typically sustain turbulent motions with vertical length scales that are small compared with the local scale height and velocity fluctuations that are small compared to the local sound speed. (The local scale height is the local e-folding scale of a background thermodynamic variable. For example, the pressure scale height in a stellar interior is $H_P \equiv (\partial_r \ln P)^{-1}$.) In this limit, the Spiegel–Veronis–Boussinesq equations are a rigorous approximation for the fluctuations of the velocity field and thermodynamic variables of a compressible fluid on top of a stably stratified background (Spiegel & Veronis 1960). The approximation effectively filters out the high frequencies of sound waves compared to the lower frequencies of IGWs and fluid motions of interest.

The governing equations for the velocity field $\boldsymbol{u}'$ and the buoyancy variable $\theta' = \alpha g T' = -\rho' g/\rho_m$ are

$$\partial_t \boldsymbol{u}' + \boldsymbol{u}' \cdot \boldsymbol{\nabla} \boldsymbol{u}' = -\frac{1}{\rho_m} \boldsymbol{\nabla} p' + \theta' \hat{z} + \nu \nabla^2 \boldsymbol{u}', \tag{2.1a}$$

$$\partial_t \theta' + \boldsymbol{u}' \cdot \boldsymbol{\nabla} \theta' = -N^2 u_z' + \kappa \nabla^2 \theta', \tag{2.1b}$$

$$\boldsymbol{\nabla} \cdot \boldsymbol{u}' = 0. \tag{2.1c}$$

Here α is the coefficient of thermal expansion, g is the local gravitational constant, T' is the temperature perturbation, ρ' is the density perturbation, ρ_m is the mean density of the region, p' is the pressure perturbation and N is the local Brunt–Väisälä frequency. Primed variables here denote dimensional quantities and unprimed variables will later denote dimensionless quantities. Note that the Brunt–Väisälä frequency captures all the relevant local thermodynamics of the medium in the Boussinesq approximation of any

https://doi.org/10.1017/jfm.2023.6 Published online by Cambridge University Press

fluid (Bois 1991). As a result, the above equations are formally equivalent to those used in geophysical fluid studies of the Earth's oceans, but with a different definition of N. For example, in the case of an ideal gas one has $N^2 = \alpha g(\partial_z \bar{T} - \partial_z T_{ad})$, while in the case of a liquid, one has $N^2 = -g\partial_z \bar{\rho}/\rho_m$, where $\partial_z \bar{\rho}$, $\partial_z \bar{T}$ and $\partial_z T_{ad}$ are the background density, background temperature and adiabatic temperature gradients, respectively.

2.2. *Geophysical regime*

A stably stratified fluid forced on a horizontal length L and velocity scale U leads to turbulence with an emergent outer vertical length l_z and velocity scale u_z set by the physical parameters of the fluid $\{N, \nu, \kappa\}$. From dimensional analysis, only three dimensionless parameters characterize the fluid: the Reynolds number $Re = UL/\nu$, the Froude number $Fr = U/NL$ and the Prandtl number $Pr = \nu/\kappa$. Understanding the scaling of the emergent outer vertical scales as well as the structure of the subsequent (anisotropic) energy cascade are important theoretical and experimental goals.

In the geophysical fluid regime where $Pr = O(1)$, evidence from theoretical arguments, simulations and experimental data strongly suggests that the outer vertical length and vertical scales are directly set by the Froude number when the viscosity is sufficiently small: $l_z \sim Fr\, L$ and $u_z \sim Fr\, U$, where l_z is often called the buoyancy length scale. Strong stratification ($Fr \ll 1$) thus leads to highly anisotropic structures of the large-scale eddies characterized by long horizontal scales and short vertical scales as well as significantly more energy in the horizontal compared to the vertical velocity components. The injected energy undergoes an anisotropic forward energy cascade at large length scales until the Ozmidov scale, an intermediate scale given by $l_O = Fr^{3/2}L$ (Brethouwer *et al.* 2007). For scales smaller than l_O, the effects of buoyancy are negligible on the fast turnover times of the eddies, and an isotropic Kolmogorov cascade operates down to the dissipation scales, which are the viscous ($l_\nu = Re^{-3/4}L$) and thermal ($l_\kappa \simeq l_\nu$) scales. The range of the isotropic cascade is set by the buoyancy Reynolds number $Rb = Re\, Fr^2$ (i.e. $l_O/l_\nu = Rb^{3/4}$) and needs to be sufficiently large in order to support the two cascades characteristic of strongly stratified turbulence (Bartello & Tobias 2013).

The horizontal and vertical scales from above in the limits $Fr \ll 1$ and $Rb \gg 1$ suggest a consistent rescaling of the Boussinesq equations using the following dimensionalization (identical to that of Billant & Chomaz (2001)):

$$\boldsymbol{u}_h' = U\boldsymbol{u}_h, \quad u_z' = Fr\, U u_z, \quad \theta' = \frac{1}{Fr}\frac{U^2}{L}\theta, \quad p' = \rho_m U^2 p, \tag{2.2a}$$

$$x' = Lx, \quad y' = Ly, \quad z' = Fr\, Lz, \quad t' = \frac{L}{U}t, \tag{2.2b}$$

where the scaling of θ' is determined by a balance of $\boldsymbol{u}' \cdot \boldsymbol{\nabla}\theta' \sim N^2 u_z'$, since thermal diffusivity is considered to be sufficiently small. Substituting the above, the Boussinesq equations become

$$\partial_t \boldsymbol{u}_h + \boldsymbol{u} \cdot \boldsymbol{\nabla}\boldsymbol{u}_h = -\boldsymbol{\nabla}_h p + \left[\frac{1}{Re}\nabla_h^2 + \frac{1}{Rb}\nabla_z^2\right]\boldsymbol{u}_h, \tag{2.3a}$$

$$Fr^2[\partial_t u_z + \boldsymbol{u} \cdot \boldsymbol{\nabla} u_z] = -\boldsymbol{\nabla}_z p + \theta + Fr^2\left[\frac{1}{Re}\nabla_h^2 + \frac{1}{Rb}\nabla_z^2\right]u_z, \tag{2.3b}$$

https://doi.org/10.1017/jfm.2023.6 Published online by Cambridge University Press

$$\partial_t \theta + \boldsymbol{u} \cdot \boldsymbol{\nabla} \theta = -u_z + \left[\frac{1}{Pr\, Re} \nabla_h^2 + \frac{1}{Pr\, Rb} \nabla_z^2 \right] \theta, \tag{2.3c}$$

$$\boldsymbol{\nabla} \cdot \boldsymbol{u} = 0, \tag{2.3d}$$

where $\boldsymbol{u}_h$ and $\boldsymbol{\nabla}_h$ denote the horizontal components of the velocity and gradient. Note that Rb and $Pr\, Rb$ act as effective Reynolds numbers in the vertical part of the momentum and thermal diffusion terms, respectively. Examination of the dominant balance to lowest order is helpful:

$$\partial_t \boldsymbol{u}_h + \boldsymbol{u} \cdot \boldsymbol{\nabla} \boldsymbol{u}_h = -\boldsymbol{\nabla}_h p, \tag{2.4a}$$

$$0 = -\nabla_z p + \theta, \tag{2.4b}$$

$$\partial_t \theta + \boldsymbol{u} \cdot \boldsymbol{\nabla} \theta = -u_z, \tag{2.4c}$$

$$\boldsymbol{\nabla} \cdot \boldsymbol{u} = 0. \tag{2.4d}$$

Advection in the horizontal momentum equation (2.4*a*) is balanced by horizontal pressure gradients, while the dominant balance in the vertical momentum equation (2.4*b*) is instead between the vertical pressure gradient and buoyancy fluctuations. These balances will change if the viscosity is increased and the vertical gradients of the momentum diffusion term become important. Further, the buoyancy equation (2.4*c*) is a balance between temperature advection and displacement of the fluid against the background stratification gradient. It is this latter balance that will change if thermal diffusion is increased and the vertical gradients of the thermal diffusion term become important, as we show in the next section.

2.3. *Transitions from the geophysical regime*

We now aim to understand when transitions occur from the regime of geophysical fluid turbulence where $Fr \ll 1$, $Rb \gg 1$ and $Pr = O(1)$. First, let us consider the better understood transition to the viscosity-affected stratified flow regime as Re is decreased with fixed Fr and $Pr = O(1)$ (Godoy-Diana, Chomaz & Billant 2004). The case of decreasing Pr turns out to behave in an analogous manner. From the perspective of the turbulent cascades, as viscosity is increased, the viscous scale will grow until it is comparable to the Ozmidov scale, $l_\nu \sim l_O$, at which point $Rb \sim 1$ and the isotropic cascade at small scales disappears (Brethouwer *et al.* 2007). This appears as a shift of the dominant balance in the horizontal momentum equation (2.3*a*) between advection and the vertical gradient of the momentum diffusivity,

$$\frac{\boldsymbol{u}' \cdot \boldsymbol{\nabla} \boldsymbol{u}_h'}{\nu \nabla_z^2 \boldsymbol{u}_h'} \sim \frac{u_z l_z}{\nu} \sim Re\, Fr^2 = Rb, \tag{2.5}$$

where vertical and horizontal advection are comparable due to the incompressibility constraint (i.e. $u_z/l_z \sim U/L$) and $l_z/L \sim u_z/U \sim Fr$ is used to estimate the vertical scales near $Rb \sim 1$. Heuristically, Rb is the ratio of the eddy turnover rate to the viscous diffusion rate at the outer vertical scales, i.e. $Rb \sim (u_z/l_z)/(\nu/l_z^2)$. For $Rb < 1$, a change of dominant balance ($\boldsymbol{u}' \cdot \boldsymbol{\nabla} \boldsymbol{u}_h' \sim \nu \nabla_z^2 \boldsymbol{u}_h'$) leads to an alternative scaling $l_z/L = Fr/Rb^{1/2}$ (usually written as $l_z/L \sim Re^{-1/2}$) where viscosity dominates the coupling of adjacent vertical layers. The same shift occurs in the buoyancy equation ($N^2 u_z' \sim \kappa \nabla_z^2 \theta'$), and the new vertical velocity scale becomes $u_z/U \sim Fr\, Rb^{1/2}$ (derived with $\theta' \sim \nabla_z p'/\rho_m$ from the unchanged dominant balance in the vertical momentum equation). This regime is often

https://doi.org/10.1017/jfm.2023.6 Published online by Cambridge University Press

reached by simulations because computational constraints limit how small the viscosity can be set. Note that the vertical scales smoothly transition from $l_z/L \sim u_z/L \sim Fr$ at $Rb = 1$ as Rb is decreased.

Returning to the physically interesting limit $Fr \ll 1$ and $Rb \gg 1$ of strongly stratified turbulence, we now consider the effect of decreasing Pr at fixed Re and Fr, equivalent to increasing the thermal diffusivity while keeping the viscosity fixed. From the perspective of the turbulent cascades, as thermal diffusivity is increased, the thermal scale $l_\kappa \sim (Pr\,Re)^{-3/4}L$ will grow until it is comparable to the Ozmidov scale $l_\kappa \sim l_O$, at which point $Pr\,Rb \sim 1$ and thermal diffusion becomes important on mesoscales that are influenced by buoyancy forces (Lignières 2019). This appears as a shift of the dominant balance *only* in the buoyancy equation (2.3*c*) between advection and the vertical gradient of thermal diffusion:

$$\frac{\boldsymbol{u}' \cdot \boldsymbol{\nabla}\theta'}{\kappa \nabla_z^2 \theta'} \sim \frac{u_z l_z}{\kappa} \equiv Pe_t. \tag{2.6}$$

Here Pe_t is the turbulent Péclet number, which can be interpreted heuristically in a similar way to Rb as the ratio of the eddy turnover rate to the thermal diffusion rate at the outer vertical scales, i.e. $Pe_t = (u_z/l_z)/(\kappa/l_z^2)$. If we use the scalings $l_z/L \sim u_z/U \sim Fr$ from the $Pr = O(1)$ regime to estimate Pe_t in the geophysical regime, we see that $Pe_t \sim Pr\,Rb$ and so the transition from $Pe_t > 1$ to $Pe_t < 1$ occurs around $Pr\,Rb \sim 1$, exactly like the $l_\kappa \sim l_O$ transition discussed above. Thus, thermal diffusion will cause a transition in turbulent regimes if $Pr\,Rb < 1$. The scalings for u_z and l_z from the $Pr\,Rb > 1$ regime will then change (the scaling for Pe_t will correspondingly change as well).

The emergent turbulent Péclet number is a more important parameter than the standard Péclet number $Pe = Pr\,Re$ (Zahn 1992; Lignières 2019; Cope, Garaud & Caulfield 2020), which measures the ratio of advection to the horizontal gradient of thermal diffusion: $(\boldsymbol{u}' \cdot \boldsymbol{\nabla}\theta')/(\kappa \nabla_h^2 \theta') \sim UL/\kappa$. This is because $Pe_t \ll Pe$ – thermal diffusion will always be more important in the vertical than the horizontal direction. In astrophysical systems, the extremely large Reynolds numbers often keep $Pe \gg 1$ despite small Prandtl numbers. As a canonical example, turbulence from horizontal shear instabilities in the solar tachocline approximately sustain $Re = O(10^{14})$ and $Pe = O(10^8)$ using $Pr = O(10^{-6})$ (Garaud 2020). Thus horizontal thermal diffusion is likely to be less important on outer scales in other stars as well. On the other hand, we find $Pr\,Rb = O(10^1)$ (and hence $Pe_t = O(10^1)$) by using $Fr \sim 3 \times 10^{-4}$ and $Rb \sim O(10^7)$. The near unity value of Pe_t shows that vertical thermal diffusion can easily become relevant in the astrophysical case (Garaud 2021), in particular, in stars with much lower Pr (down to $Pr = O(10^{-9})$ in some stars), stronger background stratification (higher N) or weaker driving (lower U or larger L). Interestingly, these values of Re, Fr and Rb are similar to those found in Earth's atmosphere (Lilly 1983; Waite, von Larcher & Williams 2014).

An important asymptotic model known as the low Péclet-number approximation is often used to study the $Pe_t < 1$ regime (Lignières 1999). It can be derived from the shift in dominant balance in the buoyancy equation. If $Pe_t \ll 1$, then the $-N^2 u_z'$ term balances $\kappa \nabla^2 \theta'$ instead of $\boldsymbol{u}' \cdot \boldsymbol{\nabla}\theta'$. In other words, to lowest order, buoyancy fluctuations are generated by vertical advection of the mean background profile while advection of the buoyancy fluctuations is unimportant because of rapid thermal diffusion. As a result, the buoyancy fluctuations can be solved for directly, $\theta' = (N^2/\kappa)\nabla^{-2} u_z'$. This is substituted back into (2.1*a*) to get a closed momentum equation:

$$\partial_t \boldsymbol{u}' + \boldsymbol{u}' \cdot \boldsymbol{\nabla}\boldsymbol{u}' = -\frac{1}{\rho_m}\boldsymbol{\nabla}p' + \frac{N^2}{\kappa}\nabla^{-2} u_z' \hat{\boldsymbol{z}} + \nu \nabla^2 \boldsymbol{u}', \quad \boldsymbol{\nabla} \cdot \boldsymbol{u}' = 0. \tag{2.7}$$

https://doi.org/10.1017/jfm.2023.6 Published online by Cambridge University Press

There are now only two dimensional parameters, N^2/κ and ν, which, alongside the imposed U and L, imply that the scaling in this limit can only be a function of the dimensionless parameters $Pe\,Fr^{-2} = Pr\,Rb/Fr^4$ and Re (Lignières 2019; Cope *et al.* 2020).

The discussion so far has argued that the geophysical regime with $Fr \ll 1$, $Rb \gg 1$ and $Pr\,Rb > 1$ can transition either to a flow dominated by viscous effects when $Rb < 1$ or to stratified turbulence modified by thermal diffusion when $Pr\,Rb < 1$. These transitions correspond to the effective Reynolds numbers of the vertical part of the momentum and thermal diffusion terms becoming smaller than unity, respectively. Our aim now is to derive a formal scaling for the astrophysically motivated $Pr\,Rb < 1$ regime with the help of the critical balance hypothesis, but first we review critical balance arguments for the geophysical $Pr\,Rb > 1$ regime.

3. Critical balance and scaling for $Pr\,Rb > 1$

We derive here the standard scaling relations for the limit of $Fr \ll 1$, $Rb \gg 1$ and $Pr\,Rb > 1$ using critical balance arguments. Consider a stably stratified fluid where energy is injected with power P at a low wavenumber $k_f = 2\pi/L$ and sustains turbulence with a kinetic energy dissipation rate $\epsilon \sim P \sim U^3/L$, where U and L are the outer horizontal velocity and length scales. Viewing anisotropic structures in the turbulence as a function of horizontal scale $k_\perp^{-1}$, the goal is to find the characteristic vertical scale $k_\parallel^{-1}$ associated with each $k_\perp$. Here $k_\parallel$ and $k_\perp$ are wavenumbers parallel and perpendicular to the direction of gravity, respectively. Such a structure will have an associated linear time scale ω^{-1} related to the wave dispersion and a nonlinear time scale τ_{NL} related to the self-straining time scale. We discuss estimation of both time scales for the $Pr\,Rb > 1$ case before applying critical balance arguments that connect $k_\perp$ and $k_\parallel$.

The Boussinesq system supports linear motions with a dispersion relation given by $\omega(k_\parallel, k_\perp)$. In the limit of arbitrarily small viscosity and thermal diffusivity, wave damping is negligible ($\nu k^2, \kappa k^2 \ll \omega$) and the linear motions are propagating waves closely approximated by adiabatic, inviscid IGWs with dispersion $\omega \approx \omega_N = Nk_\perp/k$. Because large-scale vertical motion is strongly restricted, the vertical scales are much finer than the horizontal scales, with an anisotropy at large scales quantified by $k_\perp/k_\parallel \ll 1$. The linear wave frequency is then approximately

$$\omega_N \approx \frac{Nk_\perp}{k_\parallel}. \tag{3.1}$$

On the other hand, nonlinear interactions break up eddies and transfer energy from larger to smaller scales, setting up a cascade from the forcing to the diffusive scales where the energy is dissipated. Nonlinear interactions occur via the advection term $\boldsymbol{u}\cdot\boldsymbol{\nabla u}$. Incompressibility, $\boldsymbol{\nabla}\cdot\boldsymbol{u} = 0$, requires $\boldsymbol{\nabla}_\parallel u_\parallel \sim \boldsymbol{\nabla}_\perp u_\perp$ and allows the estimate $\boldsymbol{u}\cdot\boldsymbol{\nabla u} \simeq \boldsymbol{u}_\perp\cdot\boldsymbol{\nabla u}_\perp \simeq \boldsymbol{u}_\parallel\cdot\boldsymbol{\nabla u}_\perp$, where $u_\parallel$ and $u_\perp$ are the scale-dependent vertical and horizontal velocities, respectively. The nonlinear interaction time scale using the perpendicular nonlinearity is given by

$$\tau_{NL}^{-1} \sim k_\perp u_\perp(k_\perp). \tag{3.2}$$

The scaling of τ_{NL} with $k_\perp$ can be found if a separate relation can connect $u_\perp$ and τ_{NL}. This comes from assuming that a local (in scale) cascade brings energy down from larger to smaller scales with a 'cascade time' $\tau_{cas}(k_\perp)$ that determines the energy spectrum

https://doi.org/10.1017/jfm.2023.6 Published online by Cambridge University Press

$E(k_\perp)$:

$$k_\perp E(k_\perp) \sim u_\perp^2(k_\perp) \sim \epsilon \tau_{cas}(k_\perp). \tag{3.3}$$

A relation between τ_{cas} and τ_{NL} would provide the desired $\tau_{NL}(k_\perp)$. Note that the effects of non-local energy transfer mechanisms as well as energy irreversibly lost to the buoyancy flux are not included in this cascade, but would be needed for a more detailed theory. We expect that the presented arguments should be reasonable as long as the local kinetic energy cascade comprises an $O(1)$ fraction of the total energy cascade.

In homogeneous isotropic turbulence, the only dimensional option is to set $\tau_{cas} \sim \tau_{NL}$, which results in the standard Kolmogorov scalings $u_\perp(k_\perp) \sim (\epsilon/k_\perp)^{1/3}$, $\tau_{NL} \sim (L/U)(k_\perp L)^{-2/3}$ and $E(k_\perp) \sim \epsilon^{2/3} k_\perp^{-5/3}$. In anisotropic turbulence, the two additional dimensionless parameters $k_\parallel/k_\perp$ and $\omega\tau_{NL}$ no longer constrain the system, and the energy spectrum and cascade time can be an arbitrary functions of these dimensionless groups. A further physically motivated constraint is needed.

Nazarenko & Schekochihin (2011) propose critical balance as a universal scaling conjecture for strong turbulence in anisotropic wave systems. Critical balance states that the linear propagation ω^{-1} and the nonlinear interaction time scales τ_{NL} are approximately equal, $\omega\tau_{NL} \sim 1$, on a scale-by-scale basis at all scales where the source of anisotropy is important. Physically, in essence, this is a causality argument in a system where the perpendicular nonlinearity dominates (e.g. rotating turbulence, MHD with a mean field): a fluctuation with some $k_\perp$ cannot maintain an extent longer than $k_\parallel^{-1}$ set by requiring the linear propagation time in the parallel direction to be comparable to the nonlinear breakup time in the horizontal direction. However, the causality argument is more complicated in stably stratified turbulence (Nazarenko & Schekochihin 2011) because the nonlinearity has equal strength in the parallel and perpendicular directions, $\tau_{NL} \sim k_\perp u_\perp \sim k_\parallel u_\parallel$, so one could equally argue a balance between linear propagation time in the perpendicular direction and nonlinear breakup time in the vertical direction. In either case, since the group velocity sets the propagation speed of information, the linear time scale across either the parallel or perpendicular extent of a fluctuation is $(k_\perp v_{g,\perp})^{-1} \sim (k_\parallel v_{g,\parallel})^{-1} \sim \omega_N^{-1}$. Several physical mechanisms are known to be consistent with critical balance, including zigzag (Billant & Chomaz 2000*a*,*b*) and shear instabilities (see § 4.1); however, a complete physical picture is still an area of investigation (see further discussions in Lindborg (2006)). Going forward, we assume the critical balance hypothesis and that IGWs effectively set the linear propagation time scale in the $Pr\,Rb > 1$ limit.

Critical balance removes the ambiguity in determining the cascade time scale (i.e. $\tau_{cas} \sim \tau_{NL}$), which results in a Kolmogorov spectrum for the horizontal spectrum at all scales. The vertical spectrum can then be easily determined from $E(k_\parallel)k_\parallel \sim E(k_\perp)k_\perp$ once $k_\perp$ and $k_\parallel$ are related. Applying critical balance $\omega_N \tau_{NL} \sim 1$ and rearranging gives the following relation between $k_\perp$ and $k_\parallel$:

$$k_\perp \sim \left(\frac{\epsilon}{N^3}\right) k_\parallel^3 = l_O^2 k_\parallel^3, \tag{3.4}$$

where $l_O = (\epsilon/N^3)^{1/2} = k_O^{-1}$ is the Ozmidov scale. The anisotropy $k_\perp/k_\parallel \sim (l_O k_\parallel)^2$ decreases at smaller scales until the Ozmidov scale $k^{-1} \sim l_O$, where the turbulence returns to isotropy, $k_\perp \sim k_\parallel$ and $\tau_{NL}^{-1} \sim N$. The Ozmidov scale is thus the largest horizontal scale that can overturn before restoration by buoyancy forces becomes significant. The

https://doi.org/10.1017/jfm.2023.6 Published online by Cambridge University Press

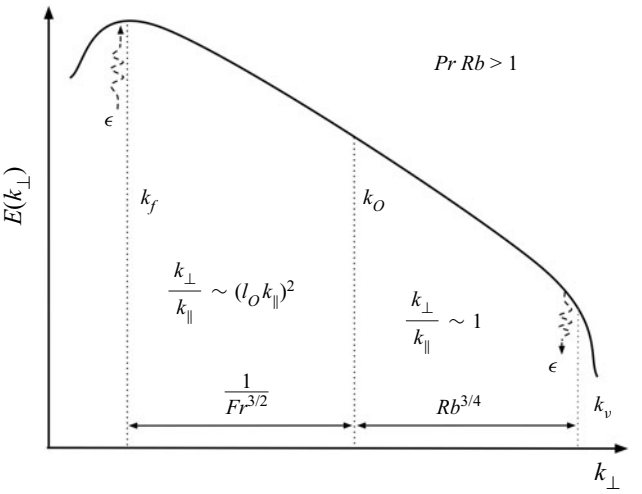

Figure 1. Energy cascade in strongly stratified turbulence for $Pr\,Rb \gg 1$ relevant to the $Pr = O(1)$ regime of Earth's atmosphere and ocean. Here $E(k_\perp)$ is the horizontal energy spectrum of the velocity field. Energy is injected at low wavenumber k_f (large scales) with power $P \sim \epsilon$ and undergoes a forward cascade down to dissipation scales. An anisotropic cascade results across horizontal wavenumbers in the range $k_f \lesssim k_\perp \lesssim k_O$, with associated vertical wavenumbers in the range $2\pi/l_z \lesssim k_\parallel \lesssim k_O$. An isotropic cascade follows for wavenumbers larger than k_O up to the dissipation wavenumber k_ν. The strength of the anisotropy is quantified by $k_\perp/k_\parallel$.

horizontal and vertical spectra for $k < k_O$ are then

$$\frac{E(k_\perp)}{U^2 L} \sim (k_\perp L)^{-5/3}, \quad \frac{E(k_\parallel)}{U^2 L} \sim Fr(k_\parallel l_z)^{-3}. \tag{3.5a,b}$$

These energy spectra agree with the theoretical scaling predictions in the geophysical literature (Dewan 1997; Billant & Chomaz 2001; Lindborg 2006), where the parallel energy spectrum is often written in a dimensional form as $E(k_\parallel) \sim N^2 k_\parallel^{-3}$.

The turbulence no longer feels the large-scale stratification gradients below the Ozmidov scale since $\omega_N \tau_{NL} \ll 1$ for $k \gg k_O$. Consequently, an isotropic Kolmogorov cascade results at small scales because τ_{NL} becomes the only dimensionally available time scale (i.e. the slow buoyancy restoration time scale is irrelevant). The isotropic cascade extends from k_O to the viscous wavenumber k_ν, where $\tau_{NL}^{-1} \sim \nu k^2 \to l_\nu \sim (\nu/\epsilon^{1/3})^{3/4}$. As a result, the vertical spectrum has a break at $k \sim k_O$ from $k_\parallel^{-3}$ to $k_\parallel^{-5/3}$, while the horizontal spectrum remains $k_\perp^{-5/3}$ throughout. The temperature thus plays an important role providing buoyancy for scales $k < k_O$ but is simply advected as a passive scalar for scales $k > k_O$ until it is dissipated at thermal diffusion scales.

For clarity, it is useful to summarize the energy cascade in terms of the dimensionless parameters Fr and Re. Energy injected at large horizontal scales L undergoes an anisotropic cascade until the Ozmidov scale, $l_O = Fr^{3/2} L$. Following the anisotropic cascade is an isotropic cascade down to the viscous scale, which can be written as $l_\nu = Re^{-3/4} L$. The size of the isotropic cascade is $l_O/l_\nu = Rb^{3/4}$. Here Rb essentially plays the role of the effective Reynolds number for the isotropic cascade with outer length scale l_O and velocity scale $u_\parallel(k_O) = (\epsilon l_O)^{1/3} = Fr^{1/2} U$ (i.e. $Rb = u_\parallel(k_O) l_O/\nu$). A schematic of the energy cascade in terms of dimensionless parameters is shown in figure 1.

https://doi.org/10.1017/jfm.2023.6 Published online by Cambridge University Press

Critical balance has provided a prediction for the anisotropy in the energy cascade for $Rb \gg 1$ and can therefore also predict the scaling of the outer vertical length and velocity scales of the system by considering the largest scales of the cascade. Substituting $k_\perp \sim 1/L$ and $k_\parallel \sim 1/l_z$ into (3.4) predicts that $l_z \sim Fr\,L$ for the outer vertical length scales. Enforcing incompressibility, $u_\parallel \sim (k_\perp/k_\parallel)u_\perp$, subsequently predicts that $u_z = u_\parallel(2\pi/L) \sim Fr\,U$ for the outer vertical velocity scale. These are exactly the scaling relations discussed in § 2.2 – critical balance successfully reproduces the known scaling relations in the $Pr\,Rb > 1$ regime.

4. Critical balance and scaling for $Pr\,Rb < 1$

We turn to deriving scaling relations in the $Pr\,Rb < 1$ regime by extending the critical balance arguments presented in the previous section. The idea is to replace the adiabatic, inviscid IGW frequency ω_N with the corresponding frequency in the low (turbulent) Péclet-number limit ω_{lPe} for the estimate of the linear time scale. A linear analysis of the Boussinesq equations with $\nu = 0$ and $\kappa \neq 0$ modelling the $Pr \ll 1$ limit gives the dispersion relation

$$\omega^2 - \mathrm{i}\omega\gamma_\kappa - \omega_N^2 = 0, \quad \gamma_\kappa = \kappa k^2, \quad \omega_N^2 = N^2\frac{k_\perp^2}{k^2}. \tag{4.1a–c}$$

In the limit $Pr\,Rb \ll 1$ (i.e. $l_\kappa \gg l_O$), thermal diffusion is faster than the restoring buoyancy time scale, so $\gamma_\kappa \gg \omega_N$ and the two roots of (4.1a–c) become $\omega \sim \mathrm{i}\omega_N^2/\gamma_\kappa$ and $\omega \sim \mathrm{i}\gamma_\kappa$. The latter is an uninteresting rapid thermal diffusion rate, while the former is an effective damping rate, $\omega_{lPe} = \mathrm{i}\omega_N^2/\gamma_\kappa = \mathrm{i}N^2k_\perp^2/\kappa k^4$ (Lignières 1999, 2019). Thus, the linear response frequency is no longer a real frequency of a restoring oscillation, but instead a damping rate γ_{lPe} (i.e. $\omega_{lPe} = \mathrm{i}\gamma_{lPe}$) corresponding to the effective rate at which restoring buoyancy and strong thermal diffusion operate. A direct linear analysis of the low turbulent Péclet-number equations (2.7) also gives the eponymous damping rate $\omega = \mathrm{i}\gamma_{lPe}$ – the two approaches nicely agree. Using the expectation of strong anisotropy at large scales $k_\perp/k_\parallel \ll 1$, the linear damping time scale can be estimated as

$$\gamma_{lPe} \sim \frac{N^2k_\perp^2}{\kappa k_\parallel^4}. \tag{4.2}$$

Before the critical balance hypothesis can be applied, a new justification is needed because the causality argument in the $Pr\,Rb > 1$ regime no longer applies: waves are overdamped rather than propagate. The instantaneous propagation of information is a peculiarity of the low Péclet-number equations (2.7), since the temperature and vertical velocity fields are coupled by an elliptic equation to lowest order. Critical balance instead becomes an argument for selective decay. The dependence between the damping rate of a fluctuation and its vertical extent, $\gamma_{lPe} \sim l_\parallel^4$ according to (4.2), means that longer vertical structures overdamp faster. As a result, any fluctuation at some $k_\perp$ with parallel extent longer than the $l_\parallel \sim k_\parallel^{-1}$ set by $\gamma_{lPe}\tau_{NL} \sim 1$ will rapidly decay away before nonlinear effects can become significant. Critical balance in the thermally diffusive regime thus determines the longest parallel structure for a given $k_\perp$ that can sustain before nonlinear breakup. A sketch of the physical argument is shown in figure 2, alongside a comparison with the causality argument in the $Pr\,Rb > 1$ regime.

https://doi.org/10.1017/jfm.2023.6 Published online by Cambridge University Press

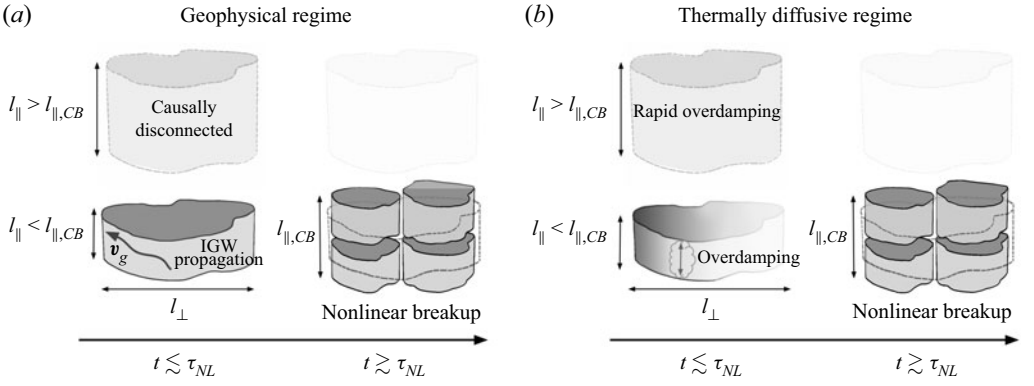

Figure 2. A sketch of the physical arguments used for critical balance for eddies with perpendicular extent $l_\perp \sim k_\perp^{-1}$. The notation $l_{\parallel,CB}$ refers to the $l_\parallel \sim k_\parallel^{-1}$ that satisfies critical balance in each regime. Panel (*a*) shows the causality argument for the geophysical regime ($Pr\,Rb > 1$). Since the group velocity, $\boldsymbol{v}_g$, of the associated IGW sets the speed at which information can propagate, any eddy with $l_\parallel > l_{\parallel,CB}$ would be causally disconnected before it nonlinearly breaks up within time $t \sim \tau_{NL}$. Panel (*b*) shows the selective decay argument for the thermally diffusive regime ($Pr\,Rb < 1$). Since the damping rate increases with $\gamma_{lPe} \sim l_\parallel^4$, any eddy with $l_\parallel > l_{\parallel,CB}$ would rapidly decay away before it could evolve.

With the modified physical interpretation, application of critical balance $\gamma_{lPe}\tau_{NL} \sim 1$ and rearrangement gives the new relationship between $k_\perp$ and $k_\parallel$ as

$$\frac{k_\perp}{k_\parallel} \sim \left(\frac{\kappa\epsilon^{1/3}}{N^2}\right)^{3/4} k_\parallel^2 = l_{OM}^2 k_\parallel^2, \tag{4.3}$$

where the modified Ozmidov scale is defined as $l_{OM} = (\kappa\epsilon^{1/3}/N^2)^{3/8}$. One can check that the critical balance prediction self-consistently maintains $\omega_N/\gamma_\kappa \ll 1$ all the way to the largest scales since $\omega_N/\gamma_\kappa \sim Nk_\perp/\kappa k_\parallel^3 \sim (Pr\,Rb)^{1/4} \ll 1$. The turbulence now returns to isotropy at the modified Ozmidov scale where the overdamping rate for a fluctuation with $k_\perp \sim k_\parallel$ is comparable to its eddy turnover time, $N^2 l_{OM}^2/\kappa \sim \tau_{NL}^{-1}$. In analogy to the Ozmidov scale, the modified Ozmidov scale is the largest horizontal scale that can overturn before overdamping becomes significant. Note that the modified Ozmidov is larger than the Ozmidov scale, as would be expected:

$$l_{OM} = \frac{Fr^{3/2}}{(Pr\,Rb)^{3/8}} L, \quad \frac{l_{OM}}{l_O} = (Pr\,Rb)^{-3/8} > 1. \tag{4.4a,b}$$

The outer vertical scale ($k_\parallel \sim l_z^{-1}$) at the largest horizontal scale where $k_\perp \sim L^{-1}$ can again be found. Subsequent enforcement of incompressibility ($\boldsymbol{\nabla} \cdot \boldsymbol{u}' = 0$) then gives $u_z \sim l_z U/L$. The result is shown below:

$$l_z \sim \frac{Fr}{(Pr\,Rb)^{1/4}} L, \quad u_z \sim \frac{Fr}{(Pr\,Rb)^{1/4}} U. \tag{4.5a,b}$$

These scalings self-consistently predict a small turbulent Péclet number $Pe_t \sim (Pr\,Rb)^{1/2} \ll 1$. At this point it becomes suggestive to define a modified Froude number

https://doi.org/10.1017/jfm.2023.6 Published online by Cambridge University Press

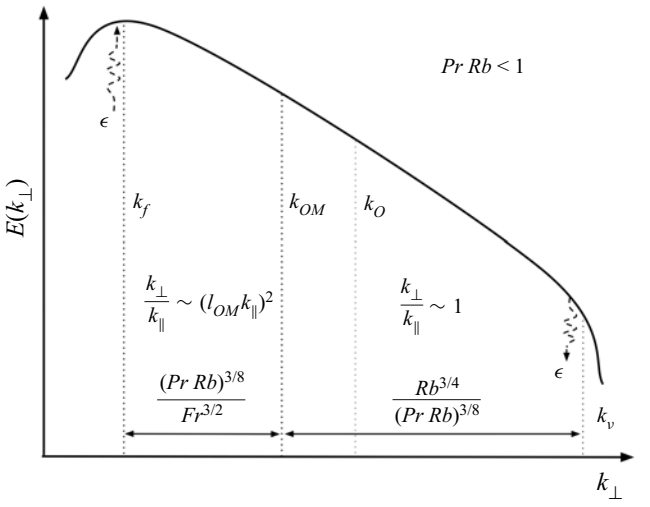

Figure 3. Energy cascade for strongly stratified turbulence for $Pr\,Rb \ll 1$ relevant to the $Pr \ll 1$ regime of stellar radiative zones. Similar to figure 1, an anisotropic cascade results in the range $k_f \lesssim k_\perp \lesssim k_{OM}$ followed by an isotropic cascade from k_{OM} to k_ν. Note that the beginning of the isotropic subrange has moved to larger scales $k_{OM} < k_O$.

as $Fr_M \equiv Fr/(Pr\,Rb)^{1/4}$ so that

$$l_z = Fr_M L, \quad l_{OM} = Fr_M^{3/2} L. \tag{4.6a,b}$$

These are the same exponents as in the geophysical regime. Using the new definition, the corresponding horizontal and vertical spectra for $k < k_{OM}$ are

$$\frac{E(k_\perp)}{U^2 L} \sim (k_\perp L)^{-5/3}, \quad \frac{E(k_\parallel)}{U^2 L} \sim Fr_M (k_\parallel l_z)^{-3}. \tag{4.7a,b}$$

The dimensional form of the parallel energy spectrum, $E(k_\parallel) \sim N(\epsilon/\kappa)^{1/2} k_\parallel^{-3}$, now depends on the dissipation and thermal diffusivity, unlike in the geophysical regime, where $E(k_\parallel) \sim N^2 k_\parallel^{-3}$. A schematic of the energy cascade is shown in figure 3, and a comparison of the cascade path in the $k_\perp$–$k_\parallel$ plane with the $Pr\,Rb > 1$ regime is shown in figure 4.

It is now clear that the transition from the $Pr\,Rb > 1$ to the $Pr\,Rb < 1$ regime simply corresponds to a replacement $Fr \to Fr_M$. How can this modified Froude number be physically understood? If the Froude number is reinterpreted to *define* the ratio of the emergent vertical length scale to the imposed horizontal scale (i.e. $l_z/L \equiv Fr$), then critical balance at the largest scales simply sets the Froude number. By substituting $k_\perp \sim L^{-1}$ and $k_\parallel \sim l_z^{-1}$ into the linear wave frequencies $\omega_N \sim N l_z/L$ and $\gamma_{lPe} \sim N^2 l_z^4/\kappa L^2$ and then comparing both with the corresponding nonlinear frequency scale $\tau_{NL}^{-1} \sim U/L$, the two Froude numbers emerge:

$$Pr\,Rb > 1: \quad \frac{l_z}{L} \sim \frac{U}{LN} \equiv Fr, \tag{4.8a}$$

$$Pr\,Rb < 1: \quad \frac{l_z}{L} \sim \left(\frac{\kappa U}{N^2 L^3}\right)^{1/4} \equiv Fr_M. \tag{4.8b}$$

https://doi.org/10.1017/jfm.2023.6 Published online by Cambridge University Press

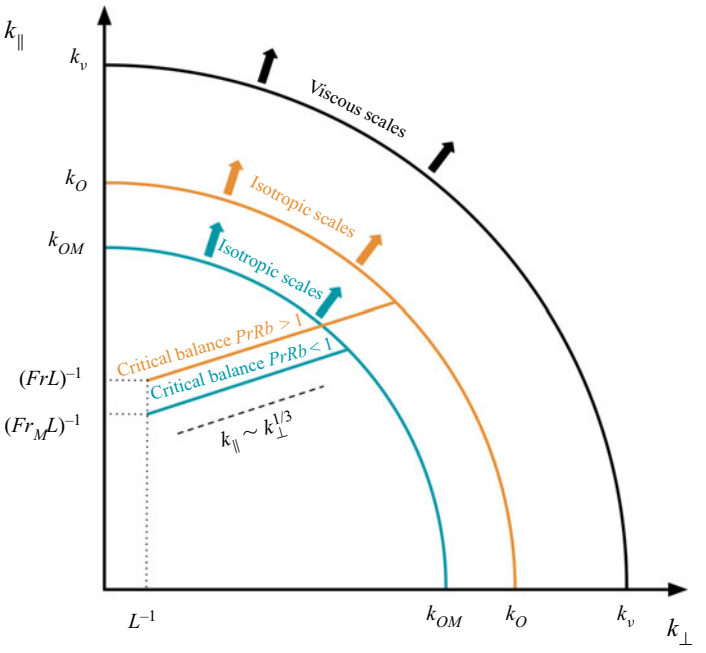

Figure 4. Comparison of the cascade path in the $k_\perp$–$k_\parallel$ plane between the geophysical (teal) and thermally diffusive (orange) regimes. Energy is injected at low perpendicular wavenumber $k_\perp \sim L^{-1}$, follows the critical balance path until the respective Ozmidov scale (k_O or k_{OM}), enters the isotropic cascade and then is dissipated at the viscous scales.

As should be expected, the outer vertical scales smoothly transition from $l_z/L = Fr$ to $l_z/L = Fr/(Pr\,Rb)^{1/4}$ at $Pr\,Rb = 1$ when Pr is decreased. This is analogous to the smooth transition from $l_z/L = Fr$ to $l_z/L = Fr/Rb^{1/2}$ at $Rb = 1$ when Re is decreased, as discussed in § 2.3. Additionally, we note that Fr_M can be rewritten in terms of $Pe\,Fr^{-2}$ and Re (i.e. $Fr_M = (Pe\,Fr^{-2})^{-1/4}$), as was required by the low turbulent Péclet-number approximation.

With the acquired scaling relations from critical balance above, we suggest the following dimensionalization for rescaling the Boussinesq equations in the $Pr\,Rb \ll 1$ limit:

$$\boldsymbol{u}_h' = U\boldsymbol{u}_h, \quad u_z' = Fr_M U u_z, \quad \theta' = \frac{1}{Fr_M}\frac{U^2}{L}\theta, \quad p' = \rho_m U^2 p, \tag{4.9a}$$

$$x' = Lx, \quad y' = Ly, \quad z' = Fr_M L z, \quad t' = \frac{L}{U}t. \tag{4.9b}$$

Aside from z' and u_z', the only other variable whose scaling changed is θ', which is now determined by the new dominant balance between $N^2 u_z' \sim \kappa \nabla_z^2 \theta'$ as discussed in § 2.3. The Boussinesq equations become

$$\partial_t \boldsymbol{u}_h + \boldsymbol{u}\cdot\boldsymbol{\nabla}\boldsymbol{u}_h = -\boldsymbol{\nabla}_h p + \left[\frac{1}{Re}\nabla_h^2 + \frac{1}{Rb_M}\nabla_z^2\right]\boldsymbol{u}_h, \tag{4.10a}$$

$$Fr_M^2[\partial_t u_z + \boldsymbol{u}\cdot\boldsymbol{\nabla}u_z] = -\nabla_z p + \theta + Fr_M^2\left[\frac{1}{Re}\nabla_h^2 + \frac{1}{Rb_M}\nabla_z^2\right]u_z, \tag{4.10b}$$

https://doi.org/10.1017/jfm.2023.6 Published online by Cambridge University Press

$$(Pr\,Rb)^{1/2}[\partial_t\theta + \boldsymbol{u}\cdot\boldsymbol{\nabla}\theta] = -u_z + \left[\frac{(Pr\,Rb)^{1/2}}{Pr\,Re}\nabla_h^2 + \nabla_z^2\right]\theta, \tag{4.10c}$$

$$\boldsymbol{\nabla}\cdot\boldsymbol{u} = 0, \tag{4.10d}$$

We see that $Rb_M \equiv Re\,Fr_M^2 = Rb/(Pr\,Rb)^{1/2}$ acts as the new effective Reynolds number and nicely matches with the scale separation between the modified Ozmidov and the viscous scale, $l_{OM}/l_\nu = (Rb_M)^{3/4}$. To lowest order,

$$\partial_t\boldsymbol{u}_h + \boldsymbol{u}\cdot\boldsymbol{\nabla}\boldsymbol{u}_h = -\boldsymbol{\nabla}_h p, \tag{4.11a}$$

$$0 = -\nabla_z p + \theta, \tag{4.11b}$$

$$0 = -u_z + \nabla_z^2\theta, \tag{4.11c}$$

$$\boldsymbol{\nabla}\cdot\boldsymbol{u} = 0, \tag{4.11d}$$

Comparing with the $Pr\,Rb > 1$ equation set (2.4), the only difference appears in the dominant balance of the buoyancy equation, where $u_z \sim \nabla_z^2\theta$ instead of $u_z \sim \boldsymbol{u}\cdot\boldsymbol{\nabla}\theta$, as expected. The vertical momentum equation remains a balance of buoyancy fluctuations with the vertical pressure gradient. Advection of the vertical momentum is now suppressed by a factor of Fr_M^2 instead of Fr^2. In principle, this term can become of order unity at sufficiently low Pr if $Pr < Fr^2/Re$; or, equivalently, when thermal diffusion is so efficient that $k_{OM} < k_f$ (or $\kappa > N^2L^3/U$), at which point the turbulence is simply isotropic.

Looking back at all the arguments so far in both the $Pr\,Rb < 1$ and $Pr\,Rb > 1$ regimes, we note the parallelism between the critical balance arguments for $\omega\tau_{NL}$ and the dominant balance arguments for the Boussinesq equations. The time scale τ_{NL} represented the nonlinear advection terms (i.e. $\boldsymbol{u}\cdot\boldsymbol{\nabla}\boldsymbol{u}_h$), while ω captured the combined effects of all the remaining linear terms. As dominant balance shifted between linear terms in various equations, ω shifted correspondingly to the dominant root of the full IGW dispersion relation (and *vice versa*). For example, $\omega_N \to \mathrm{i}\gamma_\nu \equiv \mathrm{i}\nu k_z^2$ as Re was decreased in § 2, and $\omega_N \to \omega_{lPe}$ as Pr was decreased in § 4. Critical balance and the corresponding dominant balance arguments are therefore one and the same.

4.1. *Role of vertical shear instabilities*

Examining the role of vertical shear instabilities in the turbulence offers an alternative physical interpretation of the scaling results. Many experimental and numerical studies in the geophysical regime find evidence suggesting that turbulent structures are organized to be marginally unstable to local vertical shear instabilities, a behaviour thought to be closely related to self-organized criticality (Smyth & Moum 2013; Salehipour *et al.* 2018; Smyth *et al.* 2019; Chini *et al.* 2022; Lefauve & Linden 2022). A heuristic argument for such behaviour is that the vertical shear of a turbulent eddy will generally be driven towards the marginal value of the shear for instability. An eddy with a strong vertical shear will go unstable within a dynamical time and reduce its shear to the marginal value, while one with a weak shear can become amplified to the marginal value before going unstable. As a result, vertical gradients of the horizontal velocity of eddies may be maintained at the marginal condition for vertical shear instability. As a concrete example, vertically adjacent quasi-horizontal eddy motions (e.g. 'pancake' eddies or modes) have been suggested and observed to exhibit such behaviour in early studies, such as Lin & Pao (1979), Lilly (1983), Spedding, Browand & Fincham (1996) and Riley & de BruynKops (2003) (and references therein). We now examine how the critical balance scalings in both the geophysical and

https://doi.org/10.1017/jfm.2023.6 Published online by Cambridge University Press

thermally diffusive regimes marginally satisfy the corresponding vertical shear instability criteria.

In the $Pr\,Rb > 1$ (i.e. $Pe_t \sim Pr\,Rb > 1$) regime, the nonlinear criterion to sustain turbulence in a vertical shear instability requires $J = N^2/S^2 \lesssim 1$ (Richardson 1920; Howard & Maslowe 1973) (i.e. Richardson's criterion), which is essentially based on an energy argument requiring more kinetic energy release than potential energy cost upon instability of the flow. To satisfy marginal stability, eddies with horizontal velocity scale $u_\perp(k_\perp)$ would need to maintain a vertical separation $l_\parallel$ such that $J(k_\perp) = N^2/S^2 \sim 1$ holds with $S \sim u_\perp/l_\parallel$. Indeed, substituting the critical balance results (i.e. $k_\perp E(k_\perp) \sim u_\perp^2(k_\perp)$ alongside (3.4)) into $J(k_\perp) \sim N^2 l_\parallel^2/u_\perp^2(k_\perp)$ shows that $J(k_\perp) \sim 1$ is satisfied on a scale-by-scale basis from $k_f \leq k_\perp \leq k_O$. Interpretation of strongly stratified turbulence in terms of marginal instability of local vertical shear instabilities is therefore consistent with critical balance scalings in the geophysical regime.

In the $Pr\,Rb < 1$ (i.e. $Pe_t \sim (Pr\,Rb)^{1/2} < 1$) regime, the nonlinear instability criterion is relaxed due to the weakening of the potential energy cost by the significant thermal diffusion rate at large vertical scales ($u_z/l_z < \kappa/l_z^2$ since $Pe_t < 1$). The criterion proposed on phenomenological grounds by Zahn (1992) requires $JPe_t \lesssim 1$ for instability, which smoothly connects across the $Pe_t = 1$ transition and has been approximately verified (in accessible parameter regimes) in recent numerical studies (Prat & Lignières 2013, 2014; Garaud, Gallet & Bischoff 2015; Prat *et al.* 2016; Garaud, Gagnier & Verhoeven 2017). To satisfy marginal stability, eddies with horizontal velocity scale $u_\perp(k_\perp)$ would need to maintain a vertical separation $l_\parallel$ such that $J(k_\perp)Pe_t(k_\perp) = N^2 u_\parallel l_\parallel/S^2\kappa \sim 1$. Similar to before, substituting the critical balance results (i.e. $k_\perp E(k_\perp) \sim u_\perp^2(k_\perp)$ alongside (4.3)) into $J(k_\perp)Pe_t(k_\perp)$ shows that $J(k_\perp)Pe_t(k_\perp) \sim 1$ is satisfied on a scale-by-scale basis from $k_f \leq k_\perp \leq k_{OM}$. Thus the consistent interpretation between the marginal instability of local vertical shear instabilities and critical balance scalings is maintained across the $Pe_t = 1$ transition into the thermally diffusive regime.

We note that some studies add the additional requirement $Re_t = u_z l_z/\nu > Re_{crit} \sim 10^3$ to ensure that viscous effects play no role in suppressing the nonlinear criterion for instability. Combining this assumption with $JPe_t \lesssim 1$ gives a weaker condition for instability, $JPr \lesssim (JPr)_{crit}$ (necessary, but not sufficient, since this is equivalent to $JPe_t \lesssim Re_t/Re_{crit}$). Reporting simulations in terms of JPr can be useful since it may be a proxy of $Re_t \sim (JPr)^{-1}$ (Prat *et al.* 2016). However, requiring $Re_t \gg 1$ as an additional assumption is unnecessary for strongly stratified turbulence because $Re_t \sim Rb_M \gg 1$ is already built in to the asymptotics. This is physically reasonable because the dynamics of scales larger than the modified Ozmidov scale cannot be affected by viscous effects (i.e. since $l_\nu \ll l_{OM}$).

4.2. *Comparison with previous work*

This work follows in the light of a series of simulations and an evolving discussion in Cope *et al.* (2020) and Garaud (2020) attempting to understand the complicated parameter space of $Pr < 1$ stratified turbulence driven by horizontal shear instabilities. Cope *et al.* (2020) examine the low Péclet-number limit where $Pe < 1$ and $Pe_t \ll 1$, which falls squarely into our $Pr\,Rb < 1$ regime and allows for comparison. Predictions of the vertical outer scales from critical balance ($u_z \sim Fr_M U$ and $l_z \sim Fr_M L$) are in conflict with the theoretical predictions of Cope *et al.* (2020) shown below:

$$u_z \sim Fr_M^{2/3} U, \quad l_z \sim Fr_M^{4/3} L, \tag{4.12a,b}$$

where their notation has been translated using $Fr_M = (BPe)^{-1/4}$.

https://doi.org/10.1017/jfm.2023.6 Published online by Cambridge University Press

A major source of the discrepancy arises due to different assumptions in Cope *et al.* (2020) for the dominant balance of the vertical momentum equation. Examining the proposed balances directly on the low turbulent Péclet-number equations gives a clear way to compare. The horizontal component of the momentum equation (2.7) requires the pressure to be of order unity, $p \sim U^2/L$. For the vertical component, our arguments in this work essentially balance $\boldsymbol{\nabla}_z p' \sim (N^2/\kappa)\nabla^{-2}u_z'$, which directly implies $l_z \sim Fr_M L$ by using $\nabla^{-2} \sim l_z^2$ and enforcing incompressibility, $u_z/l_z \sim U/L$, at the outer scales. The vertical advection terms are then smaller by $O(Fr_M^2)$ (see (4.10*b*)) and result in a consistent balance similar to the $Pr\,Rb > 1$ regime (see (2.3*b*)). Cope *et al.* (2020) alternatively assume a balance of vertical advection and the thermally modified buoyancy term: $\boldsymbol{u}' \cdot \boldsymbol{\nabla} u_z' \sim (N^2/\kappa)\nabla^{-2}u_z'$. This assumption leads to an inconsistency because it results in a vertical pressure gradient that is too large ($\boldsymbol{\nabla}_z p' \gg \boldsymbol{u}' \cdot \boldsymbol{\nabla} u_z'$), as discussed in § 5.2.2 of Cope *et al.* (2020). It is unclear how (4.12*a*,*b*) would smoothly transition from the $Pr\,Rb > 1$ regime, perhaps requiring an additional intermediate turbulence regime. We also note that (4.12*a*,*b*) do not satisfy the incompressibility constraint, which stems from their assumption that the horizontal and vertical length scales of the spatial derivatives are similar. This assumption may be justified in their case, where turbulence is driven in a wide band of horizontal modes by the horizontal shear instability, while our arguments suppose an idealized forcing at a single horizontal scale.

The large set of $Pe < 1$ simulations in Cope *et al.* (2020) (e.g. their figure 8) should allow differentiation between the two theoretical predictions in principle; however, the comparison is difficult because of the small differences between the fractional exponents. A detailed follow-up analysis of the simulations in light of the new critical balance predictions hopefully should resolve the question of the correct scaling relations, and will be explored in forthcoming work. It is promising that Garaud (2020) finds a sharp transition at $Pe_t \sim 1$ (as shown in her figure 3), which we interpret as the $Pr\,Rb \sim 1$ transition.

We note that Garaud (2020) predicts an additional turbulent regime for $Pr < 1$, $Pe \gg 1$ and $Pe_t > 1$. According to the critical balance framework, this falls into the $Pr\,Rb > 1$ regime, and scaling from the geophysical literature ($l_z \sim FrL$) should simply apply. Garaud (2020) instead theoretically proposes, and finds numerical evidence for, scaling relations given by $u_z/U \sim l_z/L \sim Fr^{2/3}$. Similar to our $Pr\,Rb > 1$ regime, Garaud (2020) argues that $\boldsymbol{\nabla}_z p' \sim \theta'$ and $\boldsymbol{u}' \cdot \boldsymbol{\nabla}\theta' \sim -N^2 u_z'$, but, instead of assuming incompressibility to get $l_z/L \sim Fr$, Garaud argues for a constant scaling of the time-dependent mixing efficiency to arrive at $l_z/L \sim Fr^{2/3}$, with motivation and support from her numerical results (see her figure 4). As discussed in § 4.4.4 of Garaud (2020), several factors may be at play. First, l_z may be sensitive to the method used to extract the vertical scale from simulations. For example, Lindborg (2006) use a weighted average of k_z with the energy spectrum to find a $l_z/L \sim Fr$ scaling in $Pr = 1$ simulations, while Garaud (2020) uses the vertical correlation length in her $Pr = O(10^{-1})$ simulations. The different methods correspond to different weighting functions when integrating with the energy spectrum. It would be useful to compare both diagnostics at the same Pr to resolve this possible issue. Another issue is that reaching asymptotic values of $Rb \gg 1$ while keeping $Fr \ll 1$ is computationally expensive due to a requirement for two large-scale separations between L and l_{OM} as well as l_{OM} and l_ν. Measuring scaling exponents in simulations with $Fr = O(10^{-1})$ and $Rb = O(10^1)$ may lead to transitional scaling relations (Bartello & Tobias 2013). Indeed, the arguments

https://doi.org/10.1017/jfm.2023.6 Published online by Cambridge University Press

presented in this paper and the theoretical literature, strictly speaking, only rigorously hold for the asymptotic limits of $Pr\,Rb \gg 1$ or $Pr\,Rb \ll 1$.

5. Astrophysical applications

5.1. *Diffusion coefficients*

Mixing of chemical elements in stellar interiors by stratified turbulence can have important consequences for stellar evolution, and quantifying its efficiency is essential for comparison with stellar observations (see Maeder & Meynet 2000; Salaris & Cassisi 2017; and references therein). One-dimensional stellar evolution models require an effective vertical diffusion coefficient, D_v, that is typically estimated by the product of some characteristic vertical velocity and length scales of the turbulence, i.e. $D_v \sim u_z l_z$. Which scales to choose remains an important problem and may depend on the instability that drives the turbulence. Typical choices include using the outer vertical scales or the largest isotropic scales. The scale-dependent anisotropy obtained from critical balance allows an estimate of the contribution to D_v from eddies of different scales in stratified turbulence with horizontal length scale L and vertical scale U set by some instability (e.g. shear instabilities of differential rotation). We define the scale-dependent diffusion coefficient $\tilde{D}_v(k_\parallel) = u_\parallel(k_\parallel)k_\parallel^{-1}$ from eddies of vertical length scale $k_\parallel^{-1}$ and corresponding vertical velocity scale $u_\parallel(k_\parallel)$. Using the incompressibility relation and the anisotropy relations for $k_\perp/k_\parallel$ gives

$$k_\parallel \le k_{O(M)}: \quad \frac{\tilde{D}_v(k_\parallel)}{UL} = Fr_{(M)}^2, \tag{5.1a}$$

$$k \ge k_{O(M)}: \quad \frac{\tilde{D}_v(k)}{UL} = \frac{Fr_{(M)}^2}{(k l_{O(M)})^{4/3}} \quad (k_\parallel \sim k), \tag{5.1b}$$

where $k_{O(M)}$ is defined to be k_O for $Pr\,Rb > 1$ or k_{OM} for $Pr\,Rb < 1$ (and similarly for $l_{O(M)}$ and $Fr_{(M)}$). The turbulent diffusion coefficient in principle has contributions from turbulence at all scales, but is often argued to be dominated by either the outer scales, $D_v \sim \tilde{D}_v(l_z^{-1})$, or the Ozmidov scales, $D_v \sim \tilde{D}_v(l_{O(M)}^{-1})$. The constant value of $\tilde{D}_v$ in the large-scale anisotropic subrange for $k_\parallel < k_{O(M)}$ means that one can equally use either choice, i.e. $D_v \sim u_\parallel(l_z^{-1})l_z \sim u_\parallel(l_{O(M)}^{-1})l_{O(M)}$. Thus scaling relations based on critical balance predict that $D_v \sim Fr^2 UL$ in the $Pr\,Rb > 1$ regime and $D_v \sim Fr_M^2 UL$ in the $Pr\,Rb < 1$ regime. The estimated turbulent diffusion coefficient in the $Pr\,Rb < 1$ limit is larger than in the $Pr\,Rb > 1$ limit by a factor of

$$\frac{D_v^{[Pr\,Rb<1]}}{D_v^{[Pr\,Rb>1]}} \sim \left(\frac{Fr_M}{Fr}\right)^2 = \frac{1}{(Pr\,Rb)^{1/2}}, \tag{5.2}$$

which is significant only if $Pr\,Rb \ll 1$.

The foundational work of Zahn (1992) (see also Lignières 2019) uses the modified Ozmidov scales, $D_v \sim u_\parallel(l_{OM}^{-1})l_{OM} \sim (\epsilon\kappa/N^2)^{1/2}$, in agreement with the prediction above. Our estimates for D_v, therefore, do not affect the results of previous astrophysical studies based on the estimate for D_v by Zahn (1992). Lastly, we note that the diffusion coefficient in the $Pr\,Rb < 1$ limit agrees with the prediction from Cope *et al.* (2020) (using the outer vertical scales for estimation of $D_v \sim u_\parallel(l_z^{-1})l_z$), although the agreement may be coincidental given their different predictions for u_z and l_z as discussed in § 4.2.

https://doi.org/10.1017/jfm.2023.6 Published online by Cambridge University Press

5.2. *Small-scale dynamo instability criterion*

Turbulence in the fully ionized and highly conductive plasma of a stellar radiative zone may be able to generate and sustain magnetic fields on scales smaller than the forcing scale through the small-scale dynamo (SSD). Anisotropy in the velocity field caused by stable stratification makes dynamo action less efficient compared to isotropic turbulence at the same magnetic Reynolds number, $Rm = UL/\eta$, where η is the resistivity. Indeed, the limit of infinitely strong stratification leads to a planar velocity field (i.e. $\boldsymbol{u} = (u_x(x, y, z, t), u_y(x, y, z, t), 0)$), which is a known anti-dynamo flow (Zeldovich & Ruzmaikin 1980). Using a large set of direct numerical simulations, Skoutnev, Squire & Bhattacharjee (2021) found that the SSD is unstable in the $Pr = O(1)$ regime if the scale separation of the Ozmidov scale and the magnetic resistive scale is sufficiently large. Quantitatively, this translates to requiring the magnetic buoyancy Reynolds number $Rb_m = Pm\,Rb$ to be larger than a critical value (i.e. $Rb_m > Rb_m^c$), where $Pm = \nu/\eta$ is the magnetic Prandtl number. The direct analogy to isotropic turbulence is the requirement that Rm be larger than a critical value $Rm > Rm^c$.

We propose that, in the $Pr\,Rb < 1$ regime, the SSD criterion switches to requiring a sufficient scale separation between the modified Ozmidov scale and the resistive scale. The criterion in the two regimes is then given by

$$Pr\,Rb > 1: \quad Rb_m = Pm\,Rb > Rb_m^c \tag{5.3a}$$

$$Pr\,Rb < 1: \quad Rb_{m,M} = Pm\,Rb_M = \frac{Pm\,Rb}{(Pr\,Rb)^{1/2}} > Rb_{m,M}^c. \tag{5.3b}$$

This extension naturally carries through the conjecture in Skoutnev *et al.* (2021) that the SSD only operates within the isotropic portion of the turbulent cascade. The new criterion predicts that the SSD will become more unstable as Pr is decreased at fixed Rb into the $Pr\,Rb < 1$ regime since $Rb_M > Rb$. Qualitatively, dynamo action becomes more efficient as the anisotropy caused by stratification is decreased by increased thermal diffusion.

We expect that both $Rb_m^c = Rb_m^c(Pm)$ and $Rb_{m,M}^c = Rb_{m,M}^c(Pm)$ should have a weak Pm dependence that is strongest around $Pm = O(1)$, similar to the dependence of $Rm^c(Pm)$ in the case of isotropic turbulence (Iskakov *et al.* 2007; Schekochihin *et al.* 2007). It would be reasonable that they are of comparable magnitudes, $Rb_{m,M}^c \sim Rb_m^c$, since both act as effective outer magnetic Reynolds numbers for their respective isotropic subranges.

6. Conclusion

Critical balance is a theory for strong turbulence in anisotropic wave systems that argues for a balance of linear wave and nonlinear interaction time scales to predict the scale-by-scale structure of the turbulent cascade. We have proposed that critical balance can unify the unity Pr geophysical regime and the extremely low Pr astrophysical regime of strongly stratified turbulence because both support anisotropic linear wave motions in different asymptotic limits of the IGW dispersion relation. The dispersion reduces to adiabatic inviscid IGWs in the $Pr = O(1)$ limit and to IGWs overdamped on buoyancy-modified time scales in the $Pr \ll 1$ limit. We find that a smooth transition between the two regimes occurs at $Pr\,Rb = O(1)$ as Pr is decreased, or equivalently when the turbulent Péclet number $Pe_t = u_z l_z/\kappa$ drops below order unity and shifts dominant balance in the buoyancy equation. Application of critical balance in the $Pr\,Rb < 1$ regime predicts an anisotropic cascade and scaling relations for the outer vertical scales that are identical to the geophysical regime if the Froude number, Fr, is simply replaced by

https://doi.org/10.1017/jfm.2023.6 Published online by Cambridge University Press

a modified Froude number, $Fr_M \equiv Fr/(Pr\,Rb)^{1/4}$ (e.g. the outer vertical length scale is $l_z \sim Fr_M L$). Indeed, a smooth transition occurs at $Pr\,Rb = 1$ between the two regimes.

The scaling relations from critical balance offer a theoretical framework for understanding the properties of strongly stratified turbulence in stellar radiative zones. Application to estimating the vertical turbulent diffusion coefficient in the $Pr\,Rb < 1$ regime gives the same scaling result as the original estimates of Zahn (1992), thereby validating their dimensional arguments. However, a complete understanding of strongly stratified turbulence in stellar radiative zones would need also to take into account the effects of non-local energy transfer, rotation and magnetic fields (large and small scale). In analogy with the geophysical regime, energy at large scales in the thermally diffusive regime is likely also transferred through non-local transfer mechanisms, not only through a local energy cascade as assumed in our critical balance arguments. Rotation may have a significant effect when the driving horizontal scales are sufficiently large to be influenced by Coriolis forces, which is thought to be the case in the upper solar radiative zone (Garaud 2020), for example. Similarly, large-scale magnetic fields will modify the wave dispersion relation and support magneto-internal waves, whose properties will change the nature of the turbulence presented here depending on the magnitude and direction of the large-scale field. Lastly, small-scale magnetic fields can grow in the isotropic portion of the turbulence through the small-scale dynamo if the stratification is not too strong in the $Pr\,Rb > 1$ regime (Skoutnev *et al.* 2021). We proposed a modified instability criterion for the SSD in the $Pr\,Rb < 1$ limit based on the new scaling laws. The modified instability criterion predicts a more easily excited dynamo, since thermal diffusion ameliorates the effect of stratification. Stellar stratified turbulence is, therefore, at the very least, in a saturated state of the SSD, containing small-scale magnetic fields in near equipartition with the isotropic scales of the velocity field. The effects of a saturated SSD on mixing and transport are unknown.

Acknowledgements. The author would like to thank M. Kunz for an early suggestion to explore more generally the ideas of critical balance, A. Bhattacharjee for providing intuition of their application to MHD turbulence, and P. Garaud for many insightful discussions on stratified turbulence that eventually led to this work. We also thank the referees for improvements to the physical interpretation of the results. We thank K. Whitman for illustration of the graphical abstract.

Funding. V.A.S. was supported by the Max-Planck/Princeton Center for Plasma Physics (NSF grant PHY-1804048).

Declaration of interests. The author reports no conflict of interest.

Author ORCIDs.
Valentin A. Skoutnev https://orcid.org/0000-0001-5287-498X.

References

Aerts, C., Mathis, S. & Rogers, T.M. 2019 Angular momentum transport in stellar interiors. *Annu. Rev. Astron. Astrophys.* **57**, 35–78.

Augier, P., Billant, P. & Chomaz, J.-M. 2015 Stratified turbulence forced with columnar dipoles: numerical study. *J. Fluid Mech.* **769**, 403–443.

Bartello, P. & Tobias, S.M. 2013 Sensitivity of stratified turbulence to the buoyancy Reynolds number. *J. Fluid Mech.* **725**, 1–22.

de Bruyn Kops, S.M. & Riley, J.J. 2019 The effects of stable stratification on the decay of initially isotropic homogeneous turbulence. *J. Fluid Mech.* **860**, 787–821.

Billant, P. & Chomaz, J.-M. 2000*a* Experimental evidence for a new instability of a vertical columnar vortex pair in a strongly stratified fluid. *J. Fluid Mech.* **418**, 167–188.

https://doi.org/10.1017/jfm.2023.6 Published online by Cambridge University Press

BILLANT, P. & CHOMAZ, J.-M. 2000*b* Theoretical analysis of the zigzag instability of a vertical columnar vortex pair in a strongly stratified fluid. *J. Fluid Mech.* **419**, 29–63.
BILLANT, P. & CHOMAZ, J.-M. 2001 Self-similarity of strongly stratified inviscid flows. *Phys. Fluids* **13** (6), 1645–1651.
BOIS, P.A. 1991 Asymptotic aspects of the Boussinesq approximation for gases and liquids. *Geophys. Astrophys. Fluid Dyn.* **58** (1–4), 45–55.
BRETHOUWER, G., BILLANT, P., LINDBORG, E. & CHOMAZ, J.-M. 2007 Scaling analysis and simulation of strongly stratified turbulent flows. *J. Fluid Mech.* **585**, 343–368.
CHINI, G.P., MICHEL, G., JULIEN, K., ROCHA, C.B. & COLM-CILLE, P.C. 2022 Exploiting self-organized criticality in strongly stratified turbulence. *J. Fluid Mech.* **933**, A22.
COPE, L., GARAUD, P. & CAULFIELD, C.P. 2020 The dynamics of stratified horizontal shear flows at low Péclet number. *J. Fluid Mech.* **903**, A1.
DEWAN, E. 1997 Saturated-cascade similitude theory of gravity wave spectra. *J. Geophys. Res.* **102** (D25), 29799–29817.
FALDER, M., WHITE, N.J. & CAULFIELD, C.P. 2016 Seismic imaging of rapid onset of stratified turbulence in the south Atlantic ocean. *J. Phys. Oceanogr.* **46** (4), 1023–1044.
FERNANDO, H.J.S. 1991 Turbulent mixing in stratified fluids. *Annu. Rev. Fluid Mech.* **23** (1), 455–493.
FERRARI, R. & WUNSCH, C. 2009 Ocean circulation kinetic energy: reservoirs, sources, and sinks. *Annu. Rev. Fluid Mech.* **41**, 253–282.
GARAUD, P. 2020 Horizontal shear instabilities at low Prandtl number. *Astrophys. J.* **901** (2), 146.
GARAUD, P. 2021 Journey to the center of stars: the realm of low Prandtl number fluid dynamics. *Phys. Rev. Fluids* **6** (3), 030501.
GARAUD, P., GAGNIER, D. & VERHOEVEN, J. 2017 Turbulent transport by diffusive stratified shear flows: from local to global models. I. Numerical simulations of a stratified plane Couette flow. *Astrophys. J.* **837** (2), 133.
GARAUD, P., GALLET, B. & BISCHOFF, T. 2015 The stability of stratified spatially periodic shear flows at low Péclet number. *Phys. Fluids* **27** (8), 084104.
GODOY-DIANA, R., CHOMAZ, J.-M. & BILLANT, P. 2004 Vertical length scale selection for pancake vortices in strongly stratified viscous fluids. *J. Fluid Mech.* **504**, 229–238.
GOLDREICH, P. & SRIDHAR, S. 1995 Toward a theory of interstellar turbulence. 2: strong Alfvenic turbulence. *Astrophys. J.* **438**, 763–775.
GREGG, M.C. 2021 *Ocean Mixing*. Cambridge University Press.
GREGG, M.C., D'ASARO, E.A., RILEY, J.J. & KUNZE, E. 2018 Mixing efficiency in the ocean. *Ann. Rev. Mar. Sci.* **10**, 443–473.
HOWARD, L.N. & MASLOWE, S.A. 1973 Stability of stratified shear flows. *Boundary-Layer Meteorol.* **4** (1), 511–523.
ISKAKOV, A.B., SCHEKOCHIHIN, A.A., COWLEY, S.C., MCWILLIAMS, J.C. & PROCTOR, M.R.E. 2007 Numerical demonstration of fluctuation dynamo at low magnetic Prandtl numbers. *Phys. Rev. Lett.* **98** (20), 208501.
IVEY, G.N., WINTERS, K.B. & KOSEFF, J.R. 2008 Density stratification, turbulence, but how much mixing? *Annu. Rev. Fluid Mech.* **40**, 169–184.
KHANI, S. 2018 Mixing efficiency in large-eddy simulations of stratified turbulence. *J. Fluid Mech.* **849**, 373–394.
LEFAUVE, A. & LINDEN, P.F. 2022 Experimental properties of continuously forced, shear-driven, stratified turbulence. Part 1. Mean flows, self-organisation, turbulent fractions. *J. Fluid Mech.* **937**, A34.
LEGASPI, J.D. & WAITE, M.L. 2020 Prandtl number dependence of stratified turbulence. *J. Fluid Mech.* **903**, A12.
LEGG, S. 2021 Mixing by oceanic lee waves. *Annu. Rev. Fluid Mech.* **53**, 173–201.
LIGNIÈRES, F. 1999 The small-Péclet-number approximation in stellar radiative zones. *Astron. Astrophys.* **348**, 933–939.
LIGNIÈRES, F. 2019 Turbulence in stably stratified radiative zone. arXiv:1911.07813
LILLY, D.K. 1983 Stratified turbulence and the mesoscale variability of the atmosphere. *J. Atmos. Sci.* **40** (3), 749–761.
LIN, J.-T. & PAO, Y.-H. 1979 Wakes in stratified fluids. *Annu. Rev. Fluid Mech.* **11** (1), 317–338.
LINDBORG, E. 2006 The energy cascade in a strongly stratified fluid. *J. Fluid Mech.* **550**, 207–242.
LINDBORG, E. & BRETHOUWER, G. 2007 Stratified turbulence forced in rotational and divergent modes. *J. Fluid Mech.* **586**, 83–108.
LUCAS, D., CAULFIELD, C.P. & KERSWELL, R.R. 2017 Layer formation in horizontally forced stratified turbulence: connecting exact coherent structures to linear instabilities. *J. Fluid Mech.* **832**, 409–437.

https://doi.org/10.1017/jfm.2023.6 Published online by Cambridge University Press

MAEDER, A. & MEYNET, G. 2000 The evolution of rotating stars. *Annu. Rev. Astron. Astrophys.* **38** (1), 143–190.

MAFFIOLI, A. & DAVIDSON, P.A. 2016 Dynamics of stratified turbulence decaying from a high buoyancy Reynolds number. *J. Fluid Mech.* **786**, 210–233.

MONISMITH, S.G., KOSEFF, J.R. & WHITE, B.L. 2018 Mixing efficiency in the presence of stratification: when is it constant? *Geophys. Res. Lett.* **45** (11), 5627–5634.

NAZARENKO, S.V. & SCHEKOCHIHIN, A.A. 2011 Critical balance in magnetohydrodynamic, rotating and stratified turbulence: towards a universal scaling conjecture. *J. Fluid Mech.* **677**, 134–153.

OKINO, S. & HANAZAKI, H. 2020 Direct numerical simulation of turbulence in a salt-stratified fluid. *J. Fluid Mech.* **891**, A19.

OZMIDOV, R.V. 1992 Variability of shelf and adjacent seas. *J. Mar. Syst.* **3** (4–5), 417–421.

PINSONNEAULT, M. 1997 Mixing in stars. *Annu. Rev. Astron. Astrophys.* **35** (1), 557–605.

PRAT, V., GUILET, J., VIALLET, M. & MÜLLER, E. 2016 Shear mixing in stellar radiative zones—II. Robustness of numerical simulations. *Astron. Astrophys.* **592**, A59.

PRAT, V. & LIGNIÈRES, F. 2013 Turbulent transport in radiative zones of stars. *Astron. Astrophys.* **551**, L3.

PRAT, V. & LIGNIÈRES, F. 2014 Shear mixing in stellar radiative zones—I. Effect of thermal diffusion and chemical stratification. *Astron. Astrophys.* **566**, A110.

RICHARDSON, L.F. 1920 The supply of energy from and to atmospheric eddies. *Proc. R. Soc. Lond.* A **97** (686), 354–373.

RILEY, J.J. & DE BRUYNKOPS, S.M. 2003 Dynamics of turbulence strongly influenced by buoyancy. *Phys. Fluids* **15** (7), 2047–2059.

RILEY, J.J. & LINDBORG, E. 2008 Stratified turbulence: a possible interpretation of some geophysical turbulence measurements. *J. Atmos. Sci.* **65** (7), 2416–2424.

RILEY, J.J. & LINDBORG, E. 2010 Recent progress in stratified turbulence. In *Ten Chapters in Turbulence* (ed. P.A. Davidson, Y. Kaneda & K.R. Sreenivasan), pp. 269–317. Cambridge University Press.

SALARIS, M. & CASSISI, S. 2017 Chemical element transport in stellar evolution models. *R. Soc. Open Sci.* **4** (8), 170192.

SALEHIPOUR, H., PELTIER, W.R. & CAULFIELD, C.P. 2018 Self-organized criticality of turbulence in strongly stratified mixing layers. *J. Fluid Mech.* **856**, 228–256.

SALEHIPOUR, H., PELTIER, W.R. & MASHAYEK, A. 2015 Turbulent diapycnal mixing in stratified shear flows: the influence of Prandtl number on mixing efficiency and transition at high Reynolds number. *J. Fluid Mech.* **773**, 178–223.

SCHEKOCHIHIN, A.A. 2022 MHD turbulence: a biased review. *J. Plasma Phys.* **88** (5), 155880501.

SCHEKOCHIHIN, A.A., ISKAKOV, A.B., COWLEY, S.C., MCWILLIAMS, J.C., PROCTOR, M.R.E. & YOUSEF, T.A. 2007 Fluctuation dynamo and turbulent induction at low magnetic Prandtl numbers. *New J. Phys.* **9** (8), 300.

SKOUTNEV, V., SQUIRE, J. & BHATTACHARJEE, A. 2021 Small-scale dynamo in stably stratified turbulence. *Astrophys. J.* **906** (1), 61.

SMYTH, W.D. & MOUM, J.N. 2013 Marginal instability and deep cycle turbulence in the eastern equatorial pacific ocean. *Geophys. Res. Lett.* **40** (23), 6181–6185.

SMYTH, W.D., NASH, J.D. & MOUM, J.N. 2019 Self-organized criticality in geophysical turbulence. *Sci. Rep.* **9** (1), 1–8.

SPEDDING, G.R., BROWAND, F.K. & FINCHAM, A.M. 1996 The long-time evolution of the initially turbulent wake of a sphere in a stable stratification. *Dyn. Atmos. Oceans* **23** (1-4), 171–182.

SPIEGEL, E.A. & VERONIS, G. 1960 On the Boussinesq approximation for a compressible fluid. *Astrophys. J.* **131**, 442.

THORPE, S.A. 2005 *The Turbulent Ocean*. Cambridge University Press.

WAITE, M.L. 2011 Stratified turbulence at the buoyancy scale. *Phys. Fluids* **23** (6), 066602.

WAITE, M.L. & BARTELLO, P. 2004 Stratified turbulence dominated by vortical motion. *J. Fluid Mech.* **517**, 281–308.

WAITE, M.L., VON LARCHER, T. & WILLIAMS, P. 2014 Direct numerical simulations of laboratory-scale stratified turbulence. In *Modelling Atmospheric and Oceanic Flows: Insights from Laboratory Experiments* (ed. T. von Larcher & P. Williams), American Geophysical Union.

ZAHN, J.-P. 1974 Rotational instabilities and stellar evolution. *Symposium-International Astronomical Union* **59**, 185–195.

ZAHN, J.-P. 1992 Circulation and turbulence in rotating stars. *Astron. Astrophys.* **265**, 115–132.

ZELDOVICH, Y.B. & RUZMAIKIN, A. 1980 Magnetic field of a conducting fluid in two-dimensional motion. *Zh. Eksp. Teor. Fiz.* **78**, 980–986.

https://doi.org/10.1017/jfm.2023.6 Published online by Cambridge University Press